

The study of the deformation of diaphragms by impulsive loadings is an urgent problem in view of the more and more widely used techniques of high-speed forming of sheet materials (hydroexplosive, electromagnetic, and electrohydraulic stamping). A number of papers [1, 2] have appeared on the dynamics of the deformation of elastic diaphragms. Problems of axisymmetric plastic flow under pulsed loading have been studied by the method of characteristics [3, 4]. Important applied aspects of explosive loading of diaphragms are described in [5]. We discuss the dependence of the properties of a transverse plastic wave (distortion wave) in a diaphragm on the state of stress. The motion is analyzed in an approximate formulation neglecting radial displacements along the Eulerian coordinate and the change in thickness of the diaphragm. The diaphragm material satisfies the Treska - Saint Venant yield condition. Results of experiments on hydroexplosively loaded diaphragms are presented.

### Theoretical Analysis

The equations of motion of an elastic diaphragm acted upon by a hydroexplosive pulse can be written in the form

$$\begin{aligned} rh\sigma_r \sin \alpha &= \frac{pr^2}{2} - h\mu \int r \frac{\partial^2 w}{\partial t^2} \frac{1}{\cos \alpha} dr; \\ \frac{h\sigma_r}{R_r} + \frac{h\sigma_\varphi}{R_\varphi} &= p - h\mu \frac{\partial^2 w}{\partial t^2} \cos \alpha, \end{aligned} \quad (1)$$

where  $r$  is the running distance of the point from the axis of symmetry,  $w$  is the vertical (axial) displacement,  $t$  is the time,  $\alpha$  is the angle between the normal to the diaphragm at a given point and the axis of symmetry,  $\sigma_r$  and  $\sigma_\varphi$  are the principal stresses, meridional and circumferential, respectively,  $p$  is the pressure in the pulse,  $h \equiv \text{const}$  is the thickness of the diaphragm,  $\mu$  is the density of the material, and  $R_r$  and  $R_\varphi$  are the principal radii of curvature, meridional and circumferential:

$$R_r = 1/\cos^3 \alpha \frac{\partial^2 w}{\partial r^2}; \quad R_\varphi = r/\cos \alpha \frac{\partial w}{\partial r}.$$

On the boundary of the diaphragm  $r = R$  and  $w = 0$ . The deflection  $w$  is in the direction of the negative semiaxis. After introducing the dimensionless variables  $x=r/R$ ,  $\tau = \sqrt{\sigma_0 t}/\sqrt{\mu R}$  ( $\sigma_0$  is the yield point),  $u=w/R$ ,  $\sigma_1 = \sigma_r/\sigma_0$ ,  $\sigma_2 = \sigma_\varphi/\sigma_0$ ,  $q = pR/2h\sigma_0$ , and making the corresponding transformations, system (1) can be written in the vector form [6]

$$\begin{aligned} \frac{\partial \vec{z}}{\partial x} + A \frac{\partial \vec{z}}{\partial \tau} &= \vec{b}, \\ \frac{\partial \vec{z}}{\partial x} &= \left\{ \frac{\partial u}{\partial x}, \frac{\partial \alpha}{\partial x}, \frac{\partial \sigma_1}{\partial x} \right\}, \quad \frac{\partial \vec{z}}{\partial \tau} = \left\{ \frac{\partial u}{\partial \tau}, \frac{\partial \alpha}{\partial \tau}, \frac{\partial \sigma_1}{\partial \tau} \right\}. \end{aligned}$$

$$\vec{b} = \left( 0, \left( \frac{2q}{\sigma_1 \cos \alpha} - \frac{\sigma_2}{\sigma_1 x} \operatorname{tg} \alpha \right), \left( \frac{\sigma_2 - \sigma_1}{x} \right) \right);$$

$$A = \begin{vmatrix} 0 & -\frac{1}{\cos^2 \alpha} & 0 \\ \frac{1}{\sigma_1} & 0 & 0 \\ \operatorname{tg} \alpha & 0 & 0 \end{vmatrix},$$

where  $v = \partial u / \partial \tau$ , and  $\tan \alpha = \partial u / \partial x$ . The system of equations (2) is complete, since  $\sigma_2$  is related to  $\sigma_1$  by the Treska-Saint Venant yield condition. The characteristics of the quasilinear system (2) are the eigenvalues of the matrix  $A \det \|A - \xi E\|$ , where  $E$  is the unit matrix. System (2) has the characteristics:

$$\frac{\partial \tau}{\partial x} = \xi_0 = 0, \quad \frac{\partial \tau}{\partial x} = \xi_+ = \sqrt{\frac{1}{-\sigma_1 \cos^2 \alpha}}, \quad \frac{\partial \tau}{\partial x} = \xi_- = \sqrt{\frac{1}{-\sigma_1 \cos^2 \alpha}}.$$

Using the method described in [6] the normalized eigenvectors  $\vec{l}$  of system (2) can be found and the differential form  $(\vec{l} \cdot d\vec{z})$  can be discussed. The eigenvectors have the form

$$\vec{l}_0 = \begin{pmatrix} 0 \\ -\sigma_1 \sin \alpha \\ \sqrt{\cos^2 \alpha + \sigma_1^2 \sin^2 \alpha} \\ \cos \alpha \\ \sqrt{\cos^2 \alpha + \sigma_1^2 \sin^2 \alpha} \end{pmatrix}; \quad \vec{l}_+ = \begin{pmatrix} \cos \alpha \\ \sqrt{\cos^2 \alpha - \sigma_1} \\ -\sqrt{-\sigma_1} \\ \sqrt{\cos^2 \alpha - \sigma_1} \\ 0 \end{pmatrix};$$

$$\vec{l}_- = \begin{pmatrix} \cos \alpha \\ \sqrt{\cos^2 \alpha - \sigma_1} \\ \sqrt{-\sigma_1} \\ \sqrt{\cos^2 \alpha - \sigma_1} \\ 0 \end{pmatrix}.$$

Since the differential forms  $(\vec{l}_0 \cdot d\vec{z})$ ,  $(\vec{l}_+ \cdot d\vec{z})$  and  $(\vec{l}_- \cdot d\vec{z})$  admit the integrating factors

$$\kappa_0 = 2\sigma_1 \cos \alpha \sqrt{\cos^2 \alpha + \sigma_1^2 \sin^2 \alpha}, \quad \kappa_+ = \kappa_- = \sqrt{\cos^2 \alpha - \sigma_1} \cos \alpha,$$

system (2) can be written in terms of Riemann invariants  $s$ :

$$\frac{\partial s_0}{\partial x} + \xi_0 \frac{\partial s_0}{\partial \tau} = \varphi_0 = \frac{2\sigma_2 \sigma_1}{x} - \frac{2\sigma_1^2}{x} \cos^2 \alpha - 4q\sigma \sin \alpha; \quad (3a)$$

$$\frac{\partial s}{\partial x} + \xi_+ \frac{\partial s}{\partial \tau} = \varphi_+ = \frac{2q - \sigma_2 \sin \alpha}{\sqrt{-\sigma_1 \cos^2 \alpha}}; \quad (3b)$$

$$\frac{\partial s}{\partial x} + \xi_- \frac{\partial s}{\partial \tau} = \varphi_- = \frac{\sigma_2 \sin \alpha - 2q}{\sqrt{-\sigma_1 \cos^2 \alpha}}, \quad (3c)$$

where

$$s_0 = \sigma_1^2 \cos^2 \alpha; \quad s_+ = v - \sqrt{-\sigma_1} \ln \frac{1 + \sin \alpha}{\cos \alpha};$$

$$s_- = v + \sqrt{-\sigma_1} \ln \frac{1 + \sin \alpha}{\cos \alpha}.$$

It is obvious that Eqs. (3) are relations for the characteristics:

$$\tau = \text{const}; \quad \frac{ds_0}{dx} = \varphi_0; \quad (4a)$$

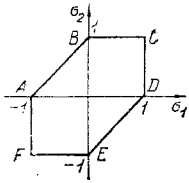


Fig. 1

The characteristic  $\xi_0 = 0$  corresponds to the instantaneous propagation of disturbances along the whole segment of the  $x$  axis  $[0; 1]$ . Forward and backward transverse waves are propagated with the velocity  $\sqrt{-\sigma_1 \cos^2 \alpha}$  along the characteristics  $\xi_+$  and  $\xi_-$ . The general form of the characteristics shows that the quasilinear system (2) is hyperbolic only for compressive stresses; i.e.,  $\sigma_1 < 0$  on the wave front. The problem is complicated by the fact that the initial conditions are specified for the characteristic  $t = 0$  (parabolic Goursat problem). The condition that system (2) be solvable [6] is that the relation

$$\cos \alpha \frac{d\sigma_1}{dx} - \sigma_1 \sin \alpha \frac{d\alpha}{dx} = \frac{\sigma_2}{x \cos \alpha} - \frac{\sigma_1 \cos \alpha}{x} - 2q \operatorname{tg} \alpha. \quad (5)$$

be satisfied on the straight line  $\tau = 0$ . Condition (5) is an expanded form of Eq. (4a) on the characteristic  $\alpha = 0$ . If  $\tau = 0$  on  $x$  for  $\tau = 0$  we obtain from (5) the equation of axisymmetric equilibrium

$$\frac{d\sigma_1}{dx} + \frac{\sigma_1 - \sigma_2}{x} = 0. \quad (6)$$

Thus the parabolic nature of the system along one characteristic is due to neglecting the Eulerian radial displacement. That contribution to the deformation which a longitudinal plastic wave would introduce is now guaranteed by an instantaneous redistribution of the stress-strain state in response to each new disturbance introduced by a transverse wave. However, the assumed simplification made it possible to write Eq. (2) in Riemann invariants, permitting a more careful investigation of the nature of the transverse plastic wave.

Plastic flow is impossible without reaching the yield point at the center or at the boundary of the diaphragm. Because of (6) the condition  $\sigma_1 = \text{const}$  leads to the equality  $\sigma_1 = \sigma_2 = \text{const}$  over the whole diaphragm. This means that for  $\alpha = 0$  and  $\sigma_1 = \text{const}$  C or F (Fig. 1) are possible states. Regime F is meaningless, since it contradicts the fact of wave propagation of compressive stresses. Regime C presupposes a discontinuity in the stress  $\sigma_1$  at the center or on the clamped boundary at  $\tau = 0$ . The constraint  $\sigma_1 < 0$  is imposed on the continuous solution of Eq. (6) for system (2) in the neighborhood of  $x = 0$  or  $x = 1$  depending on whether a forward or a backward wave is considered. We consider a backward wave propagating from the end of the interval  $x = 1$ . Since Eq. (6) continues to hold for  $\tau > 0$ , regime FA is eliminated in the neighborhood of the moving front. At the center of the diaphragm  $\sigma_1 = 1$ . Regime AB is the only possibility which need be considered in the neighborhood of the front. The solution of (6) for regime AB with the yield condition  $\sigma_2 - \sigma_1 = 1$  having the form  $\sigma_1 = \ln cx$  is not satisfied by the constraints introduced. Consequently, when the wave leaves the clamped edge (for  $\tau > 0$ ) the diaphragm is not plane in the neighborhood of the front and relations satisfying (5) are established between  $\sigma_1$  and  $\alpha$ .

The type of wave must be determined. It can be a weak shock wave or a simple wave. A discontinuous solution is possible along a characteristic or along the line on which the incoming characteristics intersect (the phase plane  $\tau x$  is considered). The possibility of a discontinuity in the solutions for  $v$ ,  $\alpha$ , and  $\sigma_1$  along a characteristic must be considered. For Eq. (3a), Eqs. (3b, c) are "residual" in the terminology of [7]. Since the residual equations involve derivatives of  $v$  and  $\alpha$  across the characteristic  $\tau = \text{const}$  discontinuities in  $v$  and  $\alpha$  are impossible, but  $\sigma_1$  can be discontinuous ( $v$  and  $\alpha$  are piecewise-continuous functions of  $\tau$ ). Similar considerations of the other two equations of system (3) lead to the conclusion that a discontinuity in  $v$ ,  $\alpha$ , or  $\sigma_1$  across the characteristic is impossible.

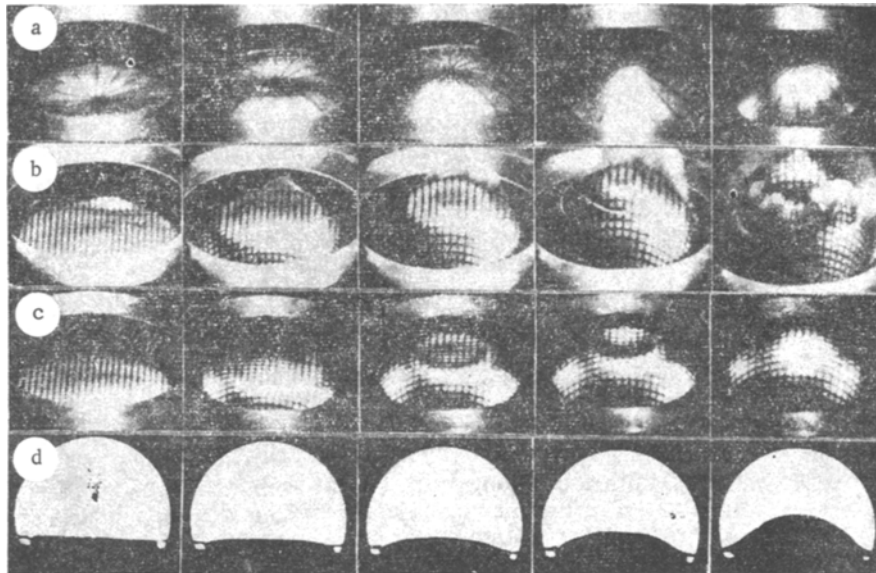


Fig. 2

The incoming characteristics intersect along the lines  $x = 0$ ,  $x = 1$ , and  $\tau = \text{const}$ . Consequently, only contact discontinuities are possible on the lines  $x = 0$  and  $x = 1$ . Thus, the distortion wave is a simple wave which can degenerate into a weak shock wave at the points  $x = 0$  and  $x = 1$ . A more concrete consideration of the question of the nature of the simple wave is difficult, since problems of the existence of a solution of the Goursat problem for a system of three quasilinear equations and the very formulation of the problem have not been developed so far. It can only be pointed out that the presence of the pressure  $p$  in system (2) eliminates self-similarity in the general case (centered waves). In the special case when the invariant  $s_0$  is constant along the characteristics  $\xi_+$  and  $\xi_-$  the solution can be a centered wave.

The deformation process can be represented qualitatively as follows. The initial conditions are  $\sigma_1 = \sigma_2 = 1$  on  $0 \leq x \leq 1$ . At  $\tau = 0$  the relations  $\sigma_1 = \sigma_2 = 1$  on  $0 \leq x < 1$  and  $\sigma_1 = \sigma_2 = -1$  on  $x = 1$  corresponding to a contact discontinuity at  $x = 1$  are established instantaneously. The diaphragm is plane at  $\tau = 0$ . For  $\tau > 0$  a deformation wave begins to propagate from the clamped edge with  $\sigma_1 = \sigma_2 = -1$  on its front. The distribution of  $\sigma_1$  is continuous between the edge and the center of the diaphragm. The stress  $\sigma_2$  on the front is discontinuous along FA. The discontinuity in  $\sigma_2$  along FA is admitted by system (2), since derivatives with respect to  $\sigma_2$  do not enter into the defining equations. The departure of the wave from the edge and the contraction of the region of state C on the diaphragm are due to the bulging of the diaphragm, satisfying (4a). As the wave approaches the center of the diaphragm it again degenerates into a weak shock wave with respect to  $\sigma_1$  (singularity at  $x = 0$ ). In this case the stresses at the center instantaneously take on the values  $\sigma_1 = \sigma_2 = 1$ .

If Eqs. (2) were not parabolic the wave process could continue to the end of the action of the pressure pulse. However, Eq. (3a) "aligns" the stress pattern irreversibly (which, in general, is peculiar to a parabolic operator) in the direction of the tensile stresses. This leads to a lowering of the intensity of the wave process and then to a transition of the hyperbolic system (2) to elliptic. After this the whole diaphragm is stretched locally. Since the stress-strain state at the instant the wave action ceases becomes the initial condition for the elliptic system, the final strain distribution must carry "wave" traces and differ from the static distribution. It is necessary to take account of the fact that the values of the residual strains are reached only while system (2) is elliptic. The wave mechanism of distortion is only one of the strain mechanisms described by the complete solution of the mixed system (2).

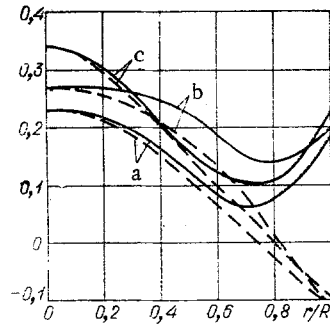


Fig. 3

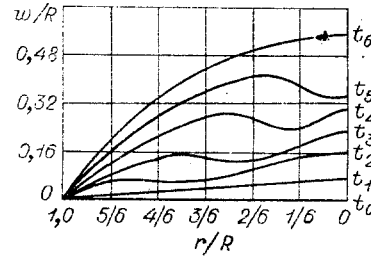


Fig. 4

### Experimental Results

A series of experiments was performed on the hydro-explosive loading of circular diaphragms of 08 kp steel, M2 copper, and AD1 aluminum in a laboratory arrangement using a test tank with rigid walls. The deformation process was recorded by taking streak photographs of a mesh ruled on the diaphragm. An accurate determination of the residual strains was made by the Moiré method. The synchronization circuit and the technique of drawing the mesh are described in [8]. Tetraerythrite pentanitrate was used as an explosive. The values of the reduction ratio of the diaphragm (the ratio of the original to the strained diameter measured from the flange) were in the 1.00-1.20 range.

Figure 2 shows motion-picture strips of the distortion process. Figure 2a illustrates the deformation of a steel sample without rupture; Figs. 2b and 2c are for copper and aluminum with rupture. Strip 2d (shadow photographs) records the deformation of a simply supported diaphragm. All the diaphragm deformation processes last  $\sim 200 \mu\text{sec}$ .

Figure 3 shows the distribution of meridional and circumferential residual strains preceding rupture for the three materials investigated.

It is clear from Fig. 2 that in a short initial period a meridian of the diaphragm is deformed as a whole. There are no moving local distortions of the surface which takes a shape close to that of a blunt cone. Then a wave of curvature of the diaphragm is propagated from the clamped edge with a clearly distinguishable ring-shaped concavity on its front. The convexity of the central part is maintained up to the instant of arrival of the ring concavity. Then the central concavity formed collapses. Figure 4 shows schematically the development of the distortion of the diaphragm. A careful study of the distortion of the ruled mesh showed that behind the front the strain waves are tensile on the front, and no distortion of the mesh is observed ahead of the front to within the accuracy of the measurements. It is therefore reasonable to assume that the ring concavity is the front of a plastic wave carrying the largest compressive stresses, and the concavity itself is accounted for by the dynamic loss of stability of shape under the action of compressive stresses. Thus, the end of the strain wave corresponding to the arrival of the plastic wave at the center of the diaphragm stops the state with the central concavity. The subsequent deformation is localized.

The distortion mechanism described above is confirmed by the dip of the residual tensile meridional strains in the middle of the segment of the x axis [0;1] (Fig. 3). In statics their distribution does not have such a singularity. In addition, it follows from Fig. 2d that the conditions on the edge do not have a substantial effect on the propagation of the distortion wave. The residual strains of a simply supported diaphragm are practically zero. Consequently, the main deformation process occurs after the disappearance of the plastic wave. But its presence affects the character of the distribution of meridional strains in the next deformation.

In conclusion, we note that the theoretical analysis developed in the first section corresponds to the actual behavior of a diaphragm under dynamic loading. The front of the plastic wave carries compressive stresses. Its clear manifestation is due to not taking account ideally of plasticity in the formulation of the problem of the dynamic loss of stabil-

ity possible on the front for  $\sigma_2 < 0$ . Equations (2) admit a discontinuity in  $\sigma_2$  so that it is possible to account for the loss of stability indirectly. Neglecting the radial displacement and inertia [making system (2) parabolic] introduces an indeterminacy into the stress distribution in the neighborhood of the front of the transverse wave. When the radial inertia is taken into account the characteristic  $\tau = \text{const}$  goes over into a family of characteristics of the longitudinal wave. The interaction of longitudinal and transverse waves leads to a rapid transition from compressive to tensile stresses. This interaction is particularly noticeable for materials that show pronounced hardening (copper). In this case there is a sharp contraction of the beam of centered waves and a rapid decrease of compressive stresses behind the front. Figure 2b confirms this conclusion: the tensile stresses behind the front and close to it lead to a rupture of the diaphragm along a parallel.

From the position taken in the present paper it is possible to account for the result in [9] that the dynamic hardening curve calculated from the values of the velocity of a transverse wave and the residual strains is the same as the static curve. Here it is necessary to take account of the fact that the wave front is related to compressive stresses and in the limiting case (excluding instability) leads to compressive strains. The residual tensile strains are determined by the nonwave period of dynamic deformation. Studies in [10] indicate an appreciable difference between the dynamic and static hardening curves for strain rates  $\sim 500 \text{ sec}^{-1}$ .

#### LITERATURE CITED

1. Kh. A. Rakhmatulin and Yu. A. Dem'yanov, Strength in Intense Short-Term Loadings [in Russian], Fizmatgiz, Moscow (1961).
2. N. Kristesku, "Dynamic plasticity," Mekhanika, Perevodov i Obz. Inostr. per Pechati, 115, No. 3 (1969).
3. B. A. Shcheglov, "Axisymmetric forming of thin-walled members by dynamic action," Mashinovedenie, No. 4 (1971).
4. B. A. Shcheglov, "Dynamics of the axisymmetric forming of thin-walled shells," in: Calculations of the Plastic Flow of Metals [in Russian], Nauka, Moscow (1973).
5. M. A. Anuchin (editor), Stamping by Explosion [in Russian], Mashinostroenie (1972).
6. B. L. Rozhdestvenskii and N. N. Yanenko, Systems of Quasilinear Equations [in Russian], Nauka, Moscow (1968).
7. A. Freidental' and Kh. Geiringer, Mathematical Theories of an Inelastic Continuous Medium [in Russian], Fizmatgiz, Moscow (1962).
8. V. N. Peretyat'ko and V. I. Bazaikin, "Techniques for investigating the dynamics of plastic deformation," Zavod. Lab., No. 12 (1973).
9. B. F. Vlasov, "Investigation of the mechanical properties of sheet copper and Duralumin in high-speed deformation processes," in: Calculations of the Processes of Plastic Flow of Metals [in Russian], Nauka, Moscow (1973).
10. V. I. Bazaikin and V. N. Peretyat'ko, "Experimental investigation of the propagation of plastic waves in copper plates," Zh. Prikl. Mekh. Tekh. Fiz., No. 1 (1974).